Effect of weathering on the engineering and petrological characteristics of metavolcanic rocks outcropping at Qusier area, Central Eastern Desert of Egypt and their utilization in construction purposes.

A. I. M. Ismail, D. Sadek Ghabrial and N. I. Abd El Ghaffar

Geological Sciences Department, National Research Centre, Dokki, Cairo, Egypt
dghabrial@yahoo.com

Abstract: This research discussed the relation between grade of weathering and engineering-petrological properties of metavolcanic rocks exposed at Bir El Beida-Wadi Zareib, Qusier area. The studied rocks are made of massive to slight sheared metabasalts, associated in places with pyroclastic deposits. They suffered greenschist to amphibolite facies metamorphism and exposed to variably weathering. According to the grade of weathering, they are classified into three groups, WI, WII and WIII, where mineralogical constituents and strength parameters changed. Chemically, moderately weathered WII samples do not show a significant effect on their composition, especially on the concentrations of the immobile elements. Most elements redistributed in their newly formed secondary minerals. The observed differences in the composition of the WII samples relative to the slightly weathered WI ones could be attributed to the fractional crystallization of melt, original magmatic features and/or crustal contamination. On the other hand, the abundances of most elements in the highly weathered WIII samples and the pyroclastic deposits display broad scatter, being commonly assigned to the weathering process that caused element redistribution, mobilization and dilution. The metavolcanic rocks are regarded to be formed in an arc setting, and derived from a mantle source that was influenced by fluids released from subduction-related component. As a result of weathering, the studied rocks exhibit changes in their microfabric and the unconfined compressive/tensile strength (Mpa) values, which are important factors in the selection of metavolcanic rocks as aggregates. The higher compressive and tensile strength data confirmed by the WI and WII Bir El Beida metavolcanics than the other weathering types in the study area, are promising to be used as aggregates in concrete according to the standard specification.

[A. I. M. Ismail, D. Sadek Ghabrial and N. I. Abd El Ghaffar. **Effect of weathering on the engineering and petrological characteristics of metavolcanic rocks outcropping at Qusier area, Central Eastern Desert of Egypt and their utilization in construction purposes.** *Life Sci J* 2014;11(10):799-813]. (ISSN:1097-8135). http://www.lifesciencesite.com. 128

Keywords: Grade of weathering, Engineering / Petrological Characters, Metavolcanic Rock Aggregates, Rock Strength

1- Introduction

Weathering process produces gradational changes in the physico-mechanical and chemical properties of the rocks and this would be assessed in quantitative rather than qualitative terms [1]. Majority of studies have provided important contributions to the classification of weathering degree of intact rock material. However, determination of weathering degree by a simple and reliable way is still open to development [2]. Recently, several studies have been tried to obtain weathering degree of rocks using simpler and more reliable methods. The weathering degree classifications can be differentiated into two main groups such as qualitative or quantitative approaches. Qualitative classifications are based on observational descriptions and results of simple index test. These are color change [3], chemical weathering degree of minerals [3, 4, 5, 6], and observational description of physical weathering degree [4, 7, 8]. On the other hand, quantitative approaches lead to consistent and objective rock weathering degree classifications more than qualitative approaches [9]. Quantitative classification approaches may consider mineralogical properties, index properties, or strength characteristics of the rocks [10, 11].

The studied rocks are mainly metavolcanics outcropping at Qusier area, central part of the Eastern Desert. Metavolcanics are widely distributed in the Eastern Desert of Egypt. They occur mostly as volcano-sedimentary successions that were previously interpreted as an early phase of eugeosynclinal filling [12]. Afterwards, the evolution of the Egyptian basement was interpreted in terms of plate tectonic models; however the basic metavolcanics were regarded as a member of ophiolites or tectonically emplaced as a remnant of oceanic crust in a mélange [13-18], while the more evolved metavolcanics were regarded to be formed in an ensimatic island arc or continental margin volcanic arc environment [19-21].

The division proposed by Stern [22] of Older Metavolcanics (OMV), Younger Metavolcanics (YMV) and Dokhan Volcanics (DV) are widely used by most investigators for the Egyptian volcanic sequences that developed in the northeastern exposure of the Arabian-Nubian Shield. OMV and YMV are restricted mainly to the central and south Eastern

Desert of Egypt (CED), where they occur below the unconformity separating the older basement units and the DV. The DV of ~ 600 Ma are dominantly high-K calc-alkaline lavas, which erupted in a post-collisional [23] or continental arc setting [24]. The DV are largely present in Sinai and the north Eastern Desert of Egypt. The OMV was described by Khalil [24] as oceanic-related volcanics and the YMV as island arc-related volcanics. Because of serve tectonics and tectonic mixing, it is not easy to distinguish the OMV from the YMV [25], and as assumed by Ali et al. [26] both metavolcanic rocks are similar expressions of the ~750 Ma crust-forming events. The ophiolitic OMV are regionally metamorphosed, low-K tholeiitic basalts, often pillowed and overlain by immature graywackes representing deep-water turbidities [27]. Island arc YMV are known as Shadli metavolcanics, calc-alkaline dominated and typically low in potash. They are made mainly of weakly metamorphosed basalts, andesites, dacites and less rhyodacites, representing more mature stage [26].

The purpose of this study is to record the changes in physico-mechanical and geochemical characteristics of different types of metavolcanic rocks and the associated pyroclastics due to weathering process, and to investigate the relationships between the texture of the rocks and engineering properties.

2. Geologic setting

The Bir El Beida-Wadi Zareib area is located between latitudes 26° 00' and 26° 11' N and longitudes 33° 56’ and 34° 02' E and is accessible by desert track from the Qift-Qusier asphaltic road. The rock units exposed at the studied area (Figure 1) belong to Pan African rock assemblage and are classified according to field relations from the oldest to the youngest as follows: Basic Metavolcanics, Acidic Metavolcanics, Metasediments, Serpentinites and related rocks, Metagabbros, Older granite, Younger granite and Nubian Sandstone.

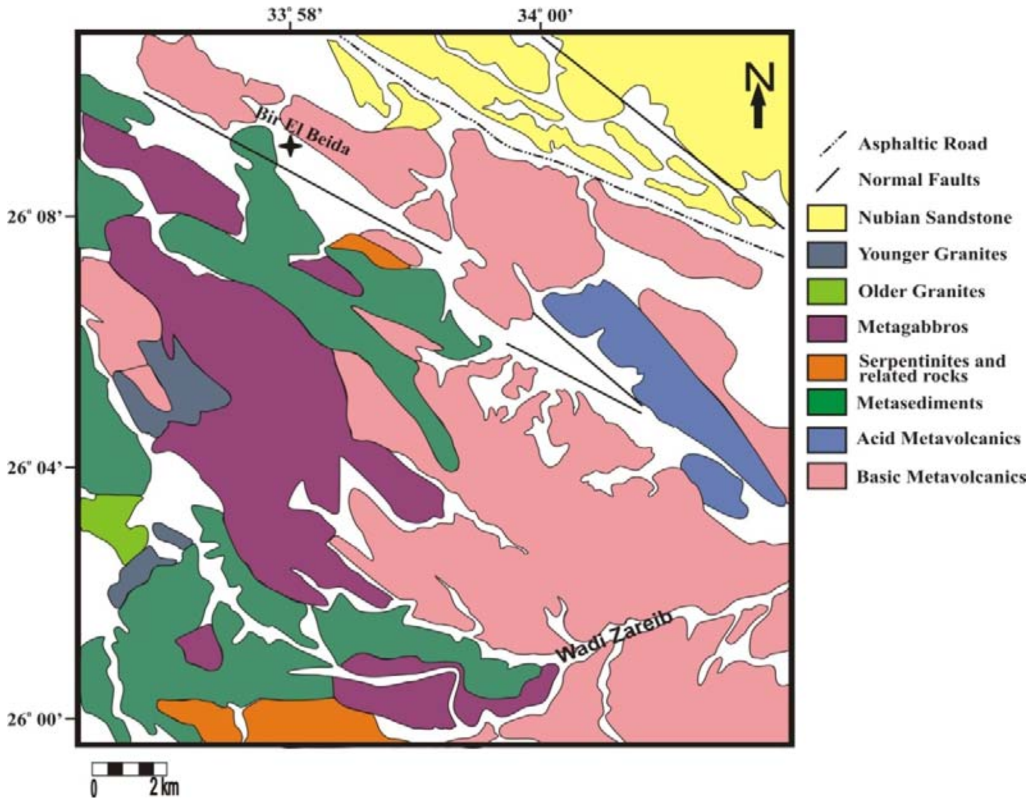

Figure 1. Geological map showing various rock units of Bir El Beida-Wadi Zareib area (modified after [28]).

The metavolcanic rocks and the associated metasediments exposed in the mapped area are capped by the metagabbros. The metavolcanics are massive to slight sheared rocks, mostly formed of fine to very fine-grained metabasalts, meta-andesites and their related pyroclastic deposits. Acidic varieties are encountered in small amounts. The studied rocks are basic metavolcanics and pyroclastic deposits. The metavolcanics are widely distributed at moderate to high elevation and were eroded to rugged hilly country. The investigated samples were collected from two localities. The northern locality, enclosing the Bir El-Beida volcanic mass, is overlain by the felsic volcanic rocks from west. The southern locality is located along Wadi Zareib and surrounded by the metagabbros from the northwest.

The basic metavolcanic rocks are characteristically dark grey, dark green to light grey and brownish green in colour; however they were variably amphibolized, chloritized and epidotized. The acidic metavolcanic rocks crop out in the eastern part of the study area and form a minor elongate belt of moderate to high elevations with rugged relief. They lay against basic metavolcanics and are dissected by mafic and felsic dikes. The acidic metavolcanic rocks are pale to yellowish gray with a reddish green tint.

The pyroclastic deposits are observed in the Wadi Zareib locality, and are rarely intercalated with banded iron oxides. They are associated with the metavolcanics forming hills of moderate relief with brownish to greenish weathering surfaces.

3. Physico-mechanical classification of weathering

There is a set of five recognition factors has been identified and used to cover all the important visual characteristics changing in the complete weathering spectrum such as discoloration and staining; texture and fabric; disintegration; decomposition and relative strength [29]. According to these recognition factors, the weathered materials were categorized into six grades (Table 1) [30-33].

Table 1. Categories and description of grades of weathering

Visual identification description	Grades
No discoloration. Minerals have a vitreous luster. Virtually no major cracks occur.	Fresh rock (W0)
No significant stained with dark grey colour. Discoloration present only along cracks. Dull luster of minerals. Minerals are tightly bonded. Few feldspars are gritty. Hair line cracks are visible in small quantity.	Slightly weathered (WI)
Slightly stained into light grey. Few minerals are gritty in appearance. Altered microcracks are visible, but they are tight. Few feldspars (plagioclase) are decomposed. Feldspar can be scratched. Discoloration observed commonly along the cracks. Increase on the extent of disintegration	Moderately weathered (WII)
Discolored and highly stained into a brown colour. Most minerals are gritty and clayey. Loosely bonded fractured grains of quartz. Microcrack is filled with clays. Few feldspars are undecomposed.	Highly weathered (WIII)
Completely discolored. Specks of white clays are present. Very loosely bonded minerals. Micro fractures are open and filled with clay and air. Sample can be crumbled by fingers.	Completely weathered (WIV)
Original texture is lost. Samples become granular with virtually no strength.	Residual soil (WV)

4. Petrography

The studied rocks comprise metabasaltic rocks, associated in places with pyroclastic deposits. The metavolcanic rocks are very fine- to fine-grained with dark grey, light grey, dark green and brownish green colour. They have been subjected to greenschist to amphibolite facies metamorphism that often caused changes in some primary minerals of the rocks. During post-metamorphic weathering, the rocks show more influence on their texture and mineralogy. The development of secondary minerals in these mafic rocks during various stages of weathering can be recognized into three types (WI, WII and WIII) with increasing the degree of weathering.

Bir El Beida metavolcanic rocks

The WI metavolcanic rocks are slightly weathered where most mafic minerals are unaltered. The rocks retain their original igneous texture and show porphyroblastic texture. They commonly contain large, corroded hornblende and plagioclase porphyroblasts embedded in a matrix of actinolite-hornblende, plagioclase and opaque minerals. Hornblende porphyroblasts occur as unhedral to subhedral crystals representing pseudomorphs after primary pyroxene. They are rarely altered to chlorite and epidote. Coarse plagioclase crystals are subhedral, slightly saussuritized and cracked; otherwise fresh plagioclase is often in the matrix and lath-shaped in form. It is also enclosed within hornblende showing an original ophitic texture.

The WII metavolcanic rocks are more weathered in which considerable amounts of mafic minerals are altered to fibrous material. Porphyroblastic texture is characteristic of these rocks where altered, resorbed plagioclase and hornblende form the porphyroblasts. Fibrous masses of acicular chlorite, white mica (sericite) and calcite commonly occur in the matrix in association with minor prismatic actinolite crystals. Hornblende porphyroblasts are highly corroded and partly or completely altered to fine grained variety of chlorite and calcite. Plagioclase porphyroblasts are fractured and showing resorption boundaries. They contain secondary products along their cleavage planes and fractures (Figure 2A). These products are mostly built up by sericite, epidote, calcite and/or clay minerals.

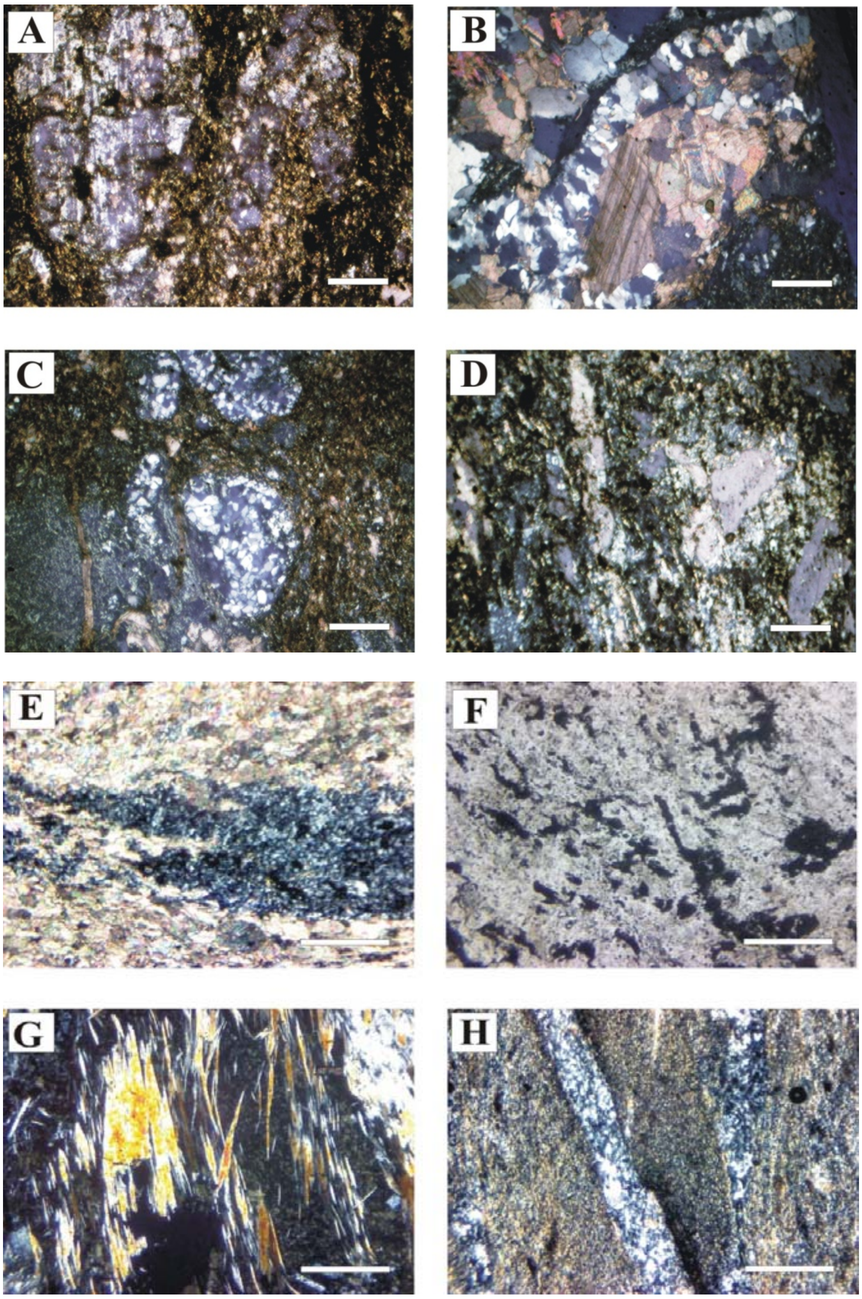

Figure 2

A- Fractured plagioclase altered along its cleavage planes and fractures to sericite, epidote and calcite in the WII metabasalts of Bir El Beida. Crossed nicols. White lines in figures (A)-(H) are 300 µm.

B- Veinlet filling with quartz and carbonates minerals in the WIII metabasalts of Bir El Beida. Crossed nicols.

C- Amphibole is replaced by authogenetic quartz in WIII metabasalts of Bir El Beida. Crossed nicols.

D- Broken plagioclase with resorption boundaries floats in a matrix of a mixture of chlorite, calcite and quartz in the WIII metabasalts of Wadi Zareib. Crossed nicols.

E- Relict serpentine in Unit 3 of Wadi Zareib pyroclastics. Crossed nicols.

F- Fe-oxide crystallized inside cracks producing veinlets in Unit 3 of Wadi Zareib pyroclastics. Plane Polarized.

G- Prismatic tremolite-actinolite and chlorite in Unit 2 of Wadi Zareib pyroclastics. Crossed nicols.

H- Quartz and calcite cut across the rock in Unit 1 of Wadi Zareib pyroclastics. Crossed nicols.

The WIII metabasalts are characterized by disappearance of original mafic minerals and by dominance of veinlets and amygdales filling with calcite and quartz (Figure 2B). In this more advanced stage of weathering, mafic minerals are completely decomposed to chlorite, talc and/or calcite with separation of iron oxides. Some of calcite crystals are mantled by opaque minerals. Authogenetic quartz also pseudomorphs after amphibole (Figure 2C). Most plagioclase porphyroblasts are totally destroyed to clayey material and calcite. The survival few plagioclase porphyroblasts are present as highly corroded, fractured crystals, which are pervasively saussuritized and their fractures are filled with chlorite and/or calcite. The matrix is characterized by parallel arrangement of chlorite and talc, which often occur either as fine-grained aggregates or as flakes.

Wadi Zareib metavolcanic rocks

The metabasalts of Wadi Zareib are obviously altered, but there are slight differences among their various weathering types that developed over the rocks. Generally, the least weathered, WI mafic rocks are made mainly of plagioclase and amphibole. Plagioclase occurs as euhedral to subhedral, prismatic crystals and is variably altered to saussurite and calcite. Amphibole (actinolite-hornblende) usually forms aggregates and sometimes contains fine plagioclase inclusions. It is sometimes replaced by fibrous of tremolite and chlorite.

As the intensity of weathering increases (WII), the original mafic minerals were fully decomposed and replaced mainly by chlorite, whereas plagioclase is strongly saussuritized and losses its euhedral shape. The rocks are traversed by few fractures filled with quartz and minor calcite.

More intensive and relatively higher rate weathering process (WIII) resulted in obliteration of the overall fabric of the rock, where remnants of plagioclase float in a matrix of an intimate mixture of chlorite, calcite and quartz (Figure 2D) cross-cutting by numerous quartz and less calcite veinlets).

Wadi Zareib pyroclastic deposits

The pyroclastic deposits associated with the Wadi Zareib mafic rocks consist of agglomerates and tuffs, often intermixed with loose clayey materials and carbonates. They are composed mainly of rock clasts and abundant secondary minerals. These deposits can be divided into three units on the basis of their mineral assemblages: unit (1) quartz + sericite + chlorite + minor calcite + minor plagioclase; unit (2) tremolite-actinolite + chlorite + dolomite + calcite + quartz + minor plagioclase; and unit (3) tremolite-actinolite + chlorite + clay minerals + opaques. Minor relicts of serpentine occur as patches (Figure 2E) between acicular tremolite-actinolite and chlorite in unit (3) suggesting pre-existing ultramafic material. This unit is affected by diffuse light brownish Fe-oxide impregnation that most probably released during decomposition of ferromagnesian minerals, and where the formation of Fe-oxide became more common, it crystallized inside cracks producing numerous veinlets (Figure 2F). Unit (2) is characterized by the common occurrence of carbonate minerals (dolomite and calcite) with quartz filling vugs and the spaces between other mineral constituents, which include few plagioclase laths, prismatic tremolite-actinolite and chlorite patches (Figure 2G). In unit (1), abundant veins filling with quartz and minor calcite were observed cutting across the rock (Figure 2H), which consists of very fine plagioclase crystals embedded in a microcrystaline matrix made of chlorite and sericite. The latter mineral grew either due to the crystallization of the intermixed clayey material or due to the strong destroying of K-feldspar-bearing felsic component but the initial shape of the replaced feldspar not preserved.

5. Geochemistry

Analyses of major oxides were carried out using an XRF Wavelength Dispersive Spectrometer (Axios Advanced, PANalytical, 2005) at the National Research Centre, Cairo, Egypt. Contents of trace and rare earth elements were determined by $LiBO_2/Li_2B_4O_7$ fusion ICP-mass spectrometry at Acme Analytical Laboratories, Canada.

As viewed by most investigators (e.g. [34-36]), except in the cases of high water/rock ratios, low grade metamorphism, weathering and hydrothermal solution do not have a major effect on the concentrations of REE, HFSE and other immobile elements (e.g. Cr, Ni). On the other hand, the fluid-mobile elements (e.g. Na, K, Rb, Ba, Sr, Ca) can be redistributed, leached from or added to the rocks during weathering. The degree of rock weathering could be evaluated by the percentages of ignition losses (L.O.I.) at 1050°C, which can be used to identify the extent of element redistribution and mobilization during variably weathering processes; however different elements exhibit different degrees of mobility. In the present study, L.O.I. is relatively low (<3 wt.%) in the slightly weathered WI samples, but the more weathered samples have higher L.O.I. reaching up to 15 wt.% in the more weathered WIII samples (Tables 2 and 3).

Bir El Beida metavolcanic rocks

The WI metabasalts of Bir El Beida contain relatively low L.O.I. (1.99-2.41 wt.%). They have a tholeiitic nature, narrow ranges of SiO_2 (44.17-45.55 wt.%), MgO (10.14-10.20 wt.%), CaO (9.90-11.85 wt.%), and low K_2O values (0.11-0.13 wt.%). In the multi-element spider diagram (Figure 3A), the samples show small enrichment in LILE (Rb, Ba, Sr), negative Nb anomalies and almost N-MORB flat HFSE, which are close to the N-MORB normalization values. The normalized REE patterns (Figure 3B; normalization C1 chondrite values after [37]) show depletion in LREE (La/Yb=0.64-0.68), insignificant Eu anomalies (Eu/Eu*=0.98-1.01) and total REE contents varying from 14.8 to 15.8 times that of chondrite.

Compared to the WI samples, the more weathered WII metabasalt is characterized by higher L.O.I. (7.38 wt.%), and shows a calc-alkaline affinity. It is more enriched in LILE and LREE (La/Yb=2.55) (Figures 3A and 3B), but it has similar or slight variation in the abundances of HFSE and HREE with very small Eu anomaly (Eu/Eu*=0.96). The mobile LILE-enriched pattern is accompanied by increase in the abundances of immobile LREE, Th, Nb, Zr and decrease in Ti, Fe, Mg contents, indicating that there is no significant elemental mobility during this stage of weathering. The observed differences between the samples of WI and WII can be assigned to the original magmatic features, crustal contamination and/or derivation of WII sample with higher SiO_2 content (47.30 wt. %) through fractional crystallization of the same basaltic magma. In the WII sample, crystallization of chlorite, sericite, calcite and clay minerals resulted in redistribution of most elements and enriched the rocks in H_2O, which dominate losses of ignition.

The highly weathered, WIII metabasalt with L.O.I. of 15.07 wt.%, shows strong depletion in major and trace elements, exception is Mg, Fe, Ni, Ca and Sr contents. In this sample, the pre-existing ferromagnesian minerals and plagioclase are pervasively altered to chlorite, talc, calcite, opaques and clayey material. This transformation led the talc and chlorite to concentrate Mg, Ni and some Fe, and calcite concentrated Ca and Sr, whereas some Si, Al and Fe migrated from these minerals towards the matrix and clayey material. Then, some of the clayey material that consisted mainly of Al and Si, is leached from the rock by fluids causing depletion in these two elements, while Fe-oxides commonly crystallized in the matrix and around altered minerals, and some silica crystallized in veinlets and amygdales as indicated by the microscopic observation of the thin-sections. The common precipitation of carbonates and silica, which have low concentration of REE and other immobile trace elements, caused depletion in total REE (ΣREE = 5.15 times of chondrite) and enriched the rocks in Ca and Sr contents.

Table 2. Major and trace element analyses for representative samples from Qusier area.

	Bir El Beida metavolcanics				Wadi Zareib metavolcanics			Wadi Zareib pyroclastics		
Grade	**WI**	**WI**	**WII**	**WIII**	**WI**	**WII**	**WIII**	**Unit 1**	**Unit 2**	**Unit 3**
SiO_2	44.17	45.55	47.3	38.16	47.9	56.47	40.19	61.92	42.00	37.37
TiO_2	1.28	1.20	1.03	0.27	0.69	0.76	1.18	0.74	0.14	1.63
Al_2O_3	13.49	13.77	16.18	5.43	15.48	13.76	14.38	13.40	14.76	12.79
Fe_2O_3	12.62	11.66	8.75	6.87	9.63	6.45	10.18	6.20	11.58	12.71
MnO	0.20	0.18	0.11	0.16	0.14	0.11	0.16	0.12	0.17	0.18
MgO	10.20	10.14	6.8	14.8	8.37	5.9	6.28	2.57	9.91	19.58
CaO	11.85	9.9	6.95	18.32	13.67	8.5	16.38	3.68	14.81	9.56
Na_2O	3.43	4.39	3.89	0.35	1.95	2.87	2.85	2.07	1.93	0.09
K_2O	0.11	0.13	0.86	0.01	0.14	0.36	0.14	2.93	0.14	0.01
P_2O_5	0.07	0.08	0.09	0.02	0.07	0.12	0.10	0.16	0.01	0.33
L.O.I.	1.99	2.41	7.38	15.07	2.85	5.32	9.09	6.65	4.61	6.25
Total	99.41	99.41	99.34	99.46	100.89	100.62	100.93	100.44	100.06	100.50
Ba	31	43	243	8	35	94	13	760	42	4
Rb	2	3	19	0.3	3.7	8.3	1.6	58.2	1.7	0.3
Sr	217	207	291	210	294	180	84	112	213	7
Y	24	23	20	6	15	18	24	17	1	30
Zr	67	70	116	23	21	56	24	12	1	100
Nb	0.9	0.8	7.5	0.7	2.3	5.7	1.0	3.5	0.1	16.4
Th	0.1	0.2	1.1	0.3	0.5	2.1	0.05	1.5	0.05	2.5
Pb	0.4	0.3	0.9	1.5	1.52	1.48	0.46	1.89	0.16	0.01
Ga	16.3	14.8	18.0	5.3	14.2	13.22	14.3	17.9	10.0	12.6
Zn	29	36	52	17	61	62	71	82	54	87
Ni	26	31	35	128	70	104	81	7	55	698
Cr	-	-	-	-	247	203	215	18	159	465
V	227	224	191	85	221	142	296	126	439	290
Co	39	39	23	29	55	36	70	25	71	66
Ta	0.05	0.05	0.5	0.05	0.2	0.4	0.1	0.2	0.05	1.1
Hf	2.2	2.2	3.1	0.7	0.7	1.7	1.0	0.5	0.01	2.4

Table 3. REE abundance (ppm) for representative samples from Qusier area.

	Bir El Beida metavolcanics				Wadi Zareib metavolcanics			Wadi Zareib pyroclastics		
Grade	**WI**	**WI**	**WII**	**WIII**	**WI**	**WII**	**WIII**	**Unit 1**	**Unit 2**	**Unit 3**
La	2.4	2.2	7.3	1.7	4.0	11.1	3.5	8	0.2	18.3
Ce	8	7.3	17.5	3.7	9.24	21.33	7.86	19.04	0.25	38.82
Pr	1.41	1.29	2.32	0.49	1.4	3.1	1.4	2.5	0.05	5.2
Nd	8.5	8.1	11.1	2.5	6.5	11.3	8.3	12.5	0.3	21.8
Sm	3	2.82	3.03	0.68	1.9	2.9	2.8	2.8	0.05	5.0
Eu	1.12	1.02	1.01	0.27	0.8	1.1	1.2	0.8	0.05	1.2
Gd	3.84	3.56	3.43	0.91	2.5	3.4	3.9	3.6	0.2	5.5
Tb	0.74	0.72	0.67	0.17	0.5	0.6	0.7	0.5	0.05	0.8
Dy	4.46	4.11	3.74	0.91	2.8	3.4	5.1	3.4	0.2	5.2
Ho	0. 93	0.87	0.76	0.21	0.6	0.7	1.1	0.7	0.05	1.1
Er	2.8	2.66	2.36	0.68	1.5	2	3.3	1.8	0.05	3.2
Tm	0.4	0.37	0.33	0.10	0.3	0.3	0.5	0.3	0.05	0.4
Yb	2.53	2.46	2.05	0.75	1.3	1.7	2.6	1.4	0.2	3.1
Lu	0.38	0.36	0.31	0.11	0.2	0.2	0.4	0.2	0.05	0.5
Total	40.51	37.84	55.91	13.18	33.54	63.13	42.66	57.54	1.75	110.12
Frequency	15.83	14.79	21.85	5.15	13.11	24.67	16.67	22.49	0.68	43.03
Eu/Eu*	1.01	0.98	0.96	1.05	1.12	1.07	1.11	0.77	1.53	0.70
La/Yb	0.68	0.64	2.55	1.63	2.21	4.68	0.97	4.10	0.72	4.23
Gd/Yb	1.26	1.20	1.38	1.00	1.59	1.65	1.24	2.13	0.83	1.47
La/Sm	0.52	0.50	1.56	1.61	1.36	2.47	0.81	1.84	2.58	2.36
La/Nb	2.67	2.75	0.97	2.43	1.52	1.95	4.00	2.29	20.00	1.12

Wadi Zareib metavolcanic rocks

The WI metabasalt of the lowest L.O.I. content (2.85 wt.%) belongs to calc-alkaline magma and displays SiO_2 content of 47.90 wt.%, and MgO, CaO and K_2O contents of 8.37, 13.67 and 0.14 wt.%, respectively. Its N-MORB-normalized trace element plot (Figure 3C) shows small enrichment in LILE with trough in Nb and a minor spike in Sr, and has almost flat HFSE, which is slightly depleted relative to the N-MORB. The REE pattern (Figure 3D) is characterized by slightly LREE-enriched (La/Yb = 2.21), with small positive Eu anomaly (Eu/Eu*= 1.12) and slightly fractionated HREE (Gd/Yb = 1.59).

In comparison with the WI metabasalt, the WII sample of calc-alkaline nature has higher L.O.I. (5.32 wt. %), SiO_2 (56.47 wt. %) and K_2O (0.36) contents and lower MgO (5.90 wt. %), Fe_2O_3 (6.45 wt. %) and CaO (8.50 wt. %) contents. In the spider diagram, it is characterized by more LILE enrichment, Nb depletion, and flat HFSE with values more or less similar to those of N-MORB (Figure 3C). The total REE show higher abundance (24.67 times that of chondrite) with more LREE enrichment (La/Yb = 4.68) (Figure 3D), but it has similar fractioned HREE pattern (Gd/Yb = 1.65) and small positive Eu anomaly (Eu/Eu*= 1.07). Such composition of the WII sample suggests that this sample might have evolved from the WI basaltic magma during fractional crystallization. The possibility of crustal contamination and/or different original magmatic features cannot be excluded. The high L.O.I. could be interpreted as a sign of predominance of chlorite; however the chloritization of amphibole enriched the chloritized parts in H_2O (L.O.I.) and resulted in removal of Ca and some Si from them to crystallize in the matrix and fractures as calcite and quartz.

The heavily weathered, WIII metabasalt has major elements concentrations similar to those of WI sample, except SiO_2 (40.19 Wt.%) and L.O.I. (9.09 Wt.%) being attributed to the decomposition of plagioclase and amphibole to chlorite and carbonates that enriched the rock in H_2O and CO_2 (L.O.I.) and impoverished it in Si, some of which might migrate out the rock. Normalized to N-MORB, less depletion in LILE was observed in WIII sample relative to WI sample, while HFSE-patterns show similarity between both samples (Figure 3C). The REE diagram shows slight LREE-depleted pattern (La/Yb = 0.97) (Figure 3D) with positive Eu anomaly (Eu/Eu*= 1.11). It has slight enrichment in the HREE, being perhaps due to the fact that the HREE are the most immobile elements, causing low in the La/Yb ratio.

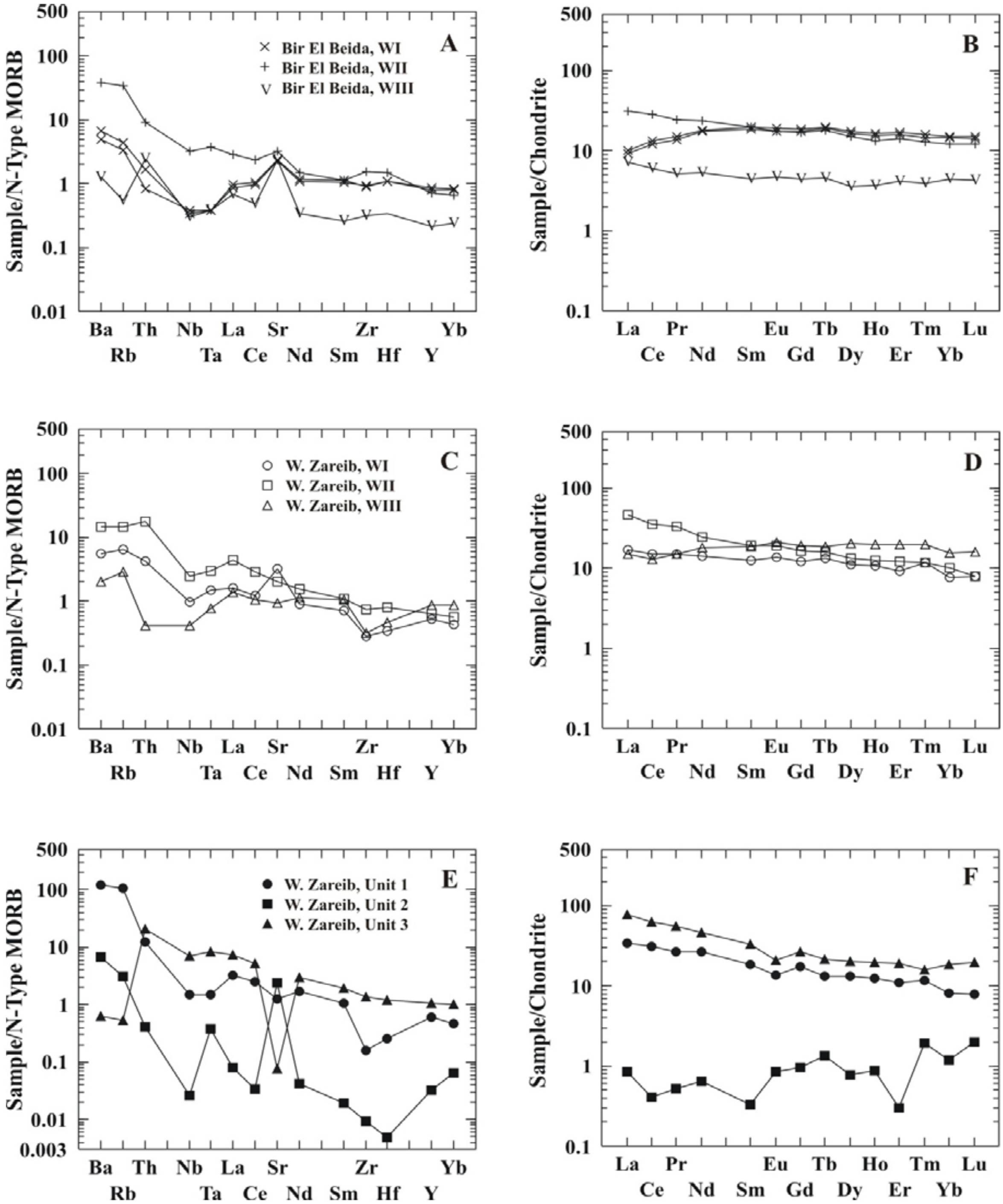

Figure 3. N-MORB-normalized trace element and chondrite-normalized REE abundance patterns for the Bir El Beida metabasalts (A&B), and Wadi Zareib metabasalts (C&D) and pyroclastics (E&F). N-MORB and chondrite normalization values after [37].

Wadi Zareib pyroclastic deposits

Analyses of pyroclastic rocks show variable major and trace element contents depending on the mineral composition of the rock units. All three units have significant L.O.I. (4.61-6.65 wt.%) contents, which are dominated in the crystal structures of chlorite, sericite and calcite formed in unit (1), tremolite, chlorite, dolomite and calcite in unit (2) and tremolite, chlorite and clay minerals in unit (3). Unit (1) with the highest SiO_2 content (61.92 wt.%), has relatively high K_2O, Ba, Rb, REE and low Fe_2O_3, MgO, CaO, Ni and Cr, whereas Unit (2) are enriched in concentrations of Fe_2O_3, MgO and CaO accompanied by increase in Ni, Cr, Sr and decrease in K_2O, Ba, Rb, REE contents. This is evident by the high proportions of quartz veins and of sericite in the matrix of unit (1) and of dolomite, tremolite and chlorite in unit (2), indicating that considerable amounts of felsic component were contained in unit (1) and of mafic component in unit (2). Unit (3) is characterized by more enrichment in concentrations of Fe_2O_3, MgO, Ni, Cr and depletion in Ba, Rb, Sr contents (Figure 3E), being consistent with the rarity of plagioclase and commence of tremolite, chlorite and opaques and suggesting presence of ultramafic component.

The REE patterns (Figure 3F) are fluctuated to mildly fractionated with La/Yb values of 4.10, 0.72 and 4.23 for unit (1), unit (2) and unit (3), respectively. The Eu/Eu* values for the three units are 0.77, 1.53 and 0.70, respectively. Unit (2) with LREE depletion, has the lowest total REE abundances (0.68 that of chondrite) because of the dilution of the rock by carbonates and quartz, which contain little REE. The dilution effect is also apparent from the low concentrations of most trace elements in multi-element diagram. Unit (3) is enriched in total REE (43.03 that of chondrite) and LREE being related most probably to the presence of clayey material characterized by high REE abundances. The mineral assemblage of unit (1) includes sericite whose crystal structure containing significant amount of REE, hence relatively enriched the rock in total REE (22.49 that of chondrite).

Tectonic setting, mantle source and the subduction component

The studied metamafic rocks suffered greenschist to amphibolite facies metamorphism and exposed to variably weathering, which might affect on the concentrations of most major element oxides and large ion lithosphile elements (LILE). Thus, the using of these elements to identify the tectonic setting of these rocks is limited. On the Zr-Y*3-Ti/100 diagram of [38] (Figure 4A), apart from highly weathered WIII and pyroclastic samples whose trace elements are relatively mobilized or diluted by carbonates and silica, most analyzed samples fall within the overlap field of MORB, IAT and CAB suggesting that the rocks were not erupted within a continental plate. Moreover, the samples are located in the field of volcanic arc basalts of the Th-Nb/16-Hf/3 diagram of [39] (Figure 4B), which also separates the Bir El Beida metabasalts of tholeiitic to calc-alkaline nature from the calc-alkaline Wadi Zareib samples. The volcanic arc setting is further documented by plotting the samples on Zr-TiO_2 of [40] (Figure 4C), and other diagrams (not shown), where they largely lie inside the field of arc lavas. Besides, the least weathered samples have La/Nb values mostly >1.2 ranging from 1.52 to 2.75, except the Bir El Beida WII sample is outside of this range (0.97), attesting a typical intra-oceanic arc setting [41, 42]. Regarding the WI metabasalts of Bir El Beida locality that are geochemically most comparable with MORB in having LREE-depleted patterns and tholeiitic affinity, but actually their K/Rb (360-457) and K/Ba (25-29) ratios are relatively low, being distinguishable from those of modern MORB, and considerably compared with modern intra-oceanic arcs such as Kermadec arc of similar REE characters [43].

As regarded by the N-MORB normalized trace elements diagrams, the samples exhibit variable LILE enrichment, Nb depletion and flat HFLE patterns, being more akin to those subduction-related magmas. To examine the role of any slab contribution to the mantle in the genesis of the present mafic rocks, we can use the concentrations of conservative (HFSE) and nonconservative (LILE and LREE) elements; however enriched of the latter elements might be added from the subducted slab to the mantle wedge. On Nb/Yb vs. Y/Yb diagram (Figure 5A), the analyzed samples fall within the mantle array after Green [44], which is defined by mantle-derived oceanic basalts, reflecting that HFSE were not important components in the subduction-related flux, as previously interpreted for the arc crust by Abd El-Rahman et al. [45] in Fawakhir area, Egypt. It is obvious that the most mafic Bir El Beida samples lie close to N-MORB indicative of a depleted mantle source, while the most mafic Wadi Zareib samples trend towards a more enriched mantle source. On the other hand, on the Nb/Yb vs. Th/Yb diagram of [46] (Figure 5B), most samples are displaced above the mantle array towards higher Th/Yb ratios implying contribution of Th from the subduction component.

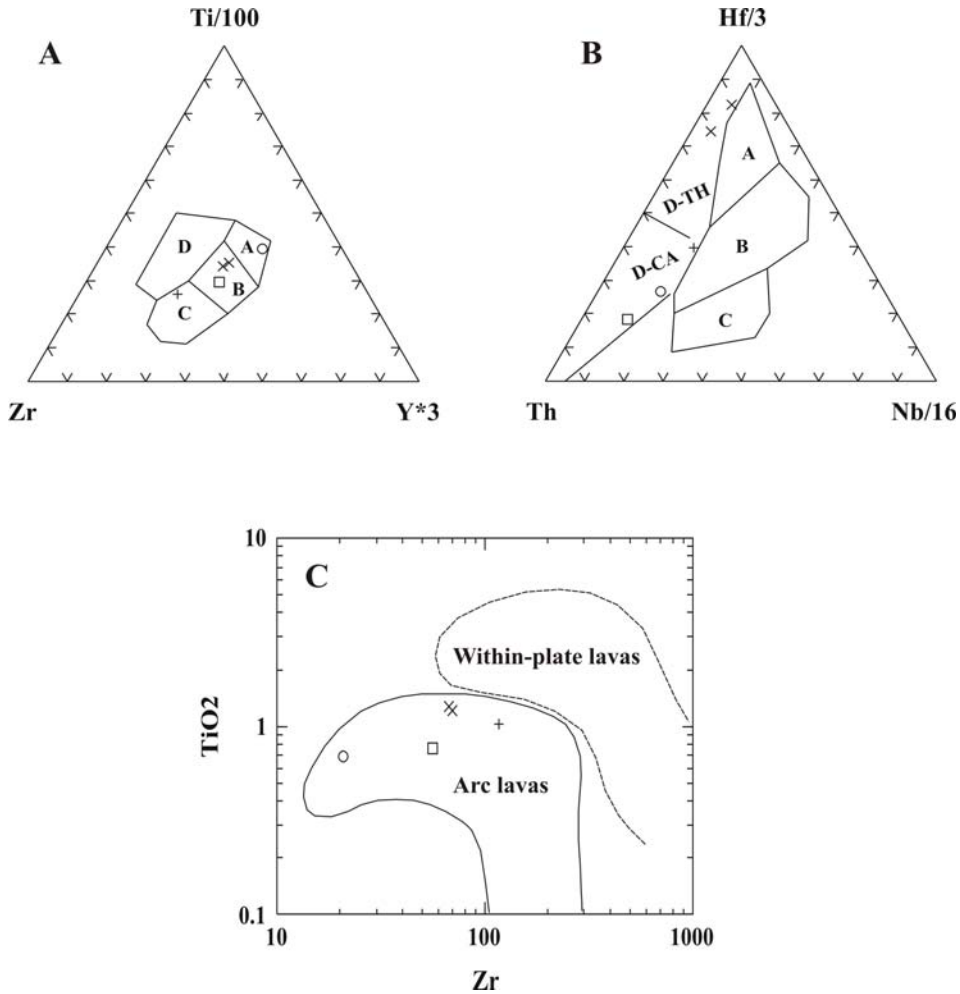

Figure 4 (A) Zr-Y-Ti diagram after [38]; A= island arc tholeiite, B= MORB, island arc tholeiite and calc-alkaline basalt, C= calc-alkaline basalt, D= within plate basalt. (B) Th-Nb-Hf diagram of [39]; A= mid-ocean ridge basalt, B= enriched mid-ocean ridge basalt, C= within-plate basalt, D-CA= calc-alkaline volcanic arc basalt, D-Th= tholeiitic volcanic arc basalt. (C) Zr vs.TiO_2 diagram of [40].

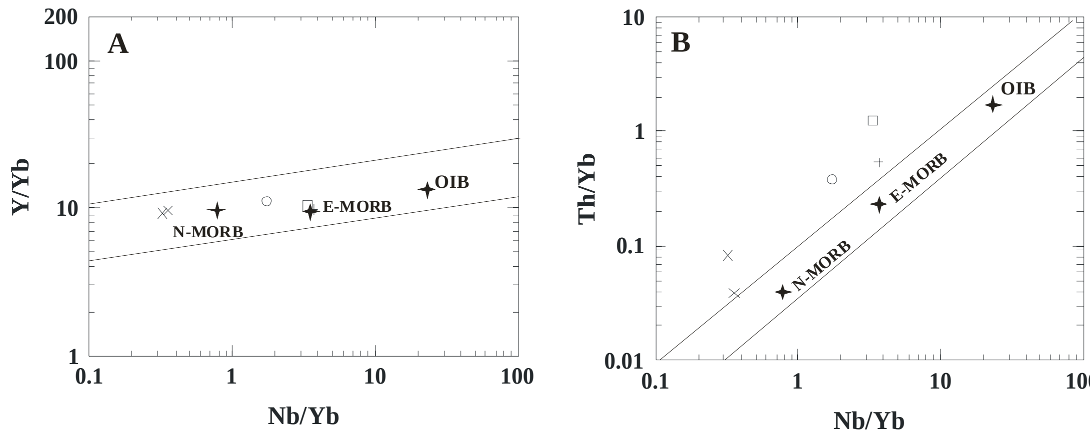

Figure 5. (A) Y/Yb vs. Nb/Yb diagram for the studied metavolcanic rocks. MORB and OIB represent the position of the mid ocean ridge and oceanic island mantle source respectively. The mantle array (MORB–OIB) after [44]. (B) Th/Yb vs. Ta/Yb diagram with mantle array after [46].

6. Relation between weathering and engineering/petrological properties

The studied rocks are classified according to the weathering classification into three groups, WI, WII and WIII (Table 4). The rock samples in the WI weathering grade show no significant staining and the minerals tightly bonded as well as few feldspar crystals are gritty and hair line cracks are visible in small quantity. In the WII weathering grade, the rocks under study are slightly stained and few minerals are gritty in appearance, and plagioclase crystals are partially decomposed. The rocks belonging to WIII weathering is discolored and stained into brownish green colour. Their minerals mostly weathered, most feldspar crystals are decomposed and secondary products commonly fill the microcracks. The petrographic characteristics such as rock texture including size, shape, arrangement/nature of minerals and degree of their interlocking play an important role in determining the rock strength and durability [47-52].

As the weathering increases, the solubility rate increases and the colour of the rocks under study changes especially along microfractures. Besides, the rocks show changes in microfabric due to the weathering process. To investigate the effect of degree of weathering on the engineering behaviour of rocks, the unconfined compressive strength (Mpa) values of the rocks in different weathering grade were determined (Table 4 and Figure 6). Gupta and Rao [1] noted that the uniaxial compressive strength values do not correspond with the order of the quartz content in the rocks. This suggests that factors other than quartz content are more important in controlling the strength behaviour. However, textural features such as microfractures, pores and voids are dominant factors in determining the strength of the rock materials. Both mineralogical and textural changes made by the weathering play a major role in governing the strength and deformational behaviour of rocks. Hussin and Poole [53] studied the role played by intragranular textures (mineral assemblage, grain size and grain boundaries) in influencing the physical properties of the aggregates and detected that they are potentially significant to the fact that such textural variation may complicate the aggregate strength.

Table 4. Relation between the rate of weathering and mineral contents as well as Unified Compressive Strength (UCS, Mpa) of the studied rocks.

Bir El Beida metavolcanics			Wadi Zareib metavolcanics			Wadi Zareib pyroclastics		
Grade	**Mineralogy**	**UCS Mpa**	**Grade**	**Mineralogy**	**UCS Mpa**	**Units**	**Mineralogy**	**UCS Mpa**
W I	Hb, Pl, Chl, Opq	85	**W I**	Hb, Pl, Chl, Qz, Opq	62	**Unit 1**	Chl, Ser, Qz, Pl, Cal, Opq	53
WII	Hb, Pl, Chl, Ser, Cal, Opq	72	**WII**	Chl, Pl, Qz, Cal, Opq	48	**Unit 2**	Tr-Act, Chl, Dol, Cal, Qz, Pl, Opq	41
WIII	Chl, Tlc, Cal, Qz, Pl, Opq	38	**WIII**	Chl, Cal, Qz, Pl, Opq	25	**Unit 3**	Tr-Act, Chl, Opq, Clay	20

Hb= hornblende, Tr-Act= tremolite-actinolite, Chl= chlorite, Tlc= talc, Pl= plagioclase, Qz= quartz, Ser= sericite, Cal= calcite, Dol= dolomite, Opq= opaque minerals, Clay= clay minerals

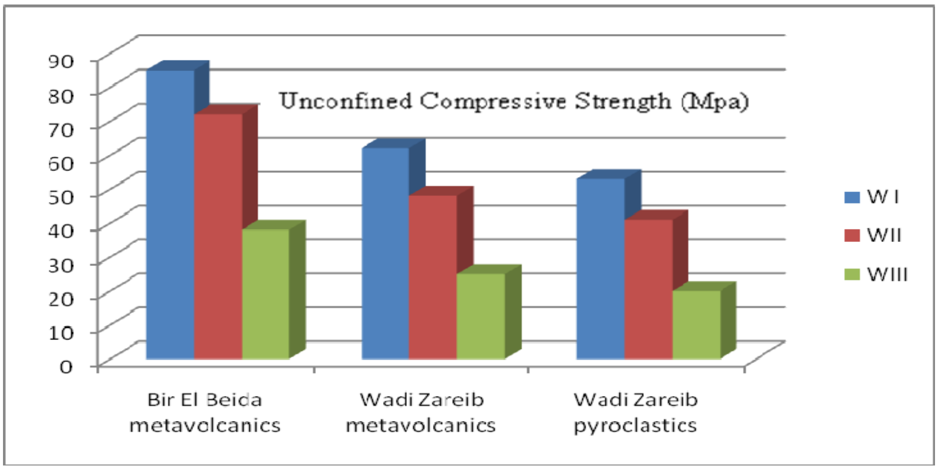

Figure 6. Unconfined Compressive Strength at different grade of weathering in the studied area.

7. The selection of aggregates according to the grade of weathering

The uniaxial compressive strength is considered as the most reliable index for strength and deformability estimation of the rocks. The weathering results in significant reduction in the compressive strength of rocks (Table 4 and Figure 6). It was observed that the rock material becomes more porous, soft, friable and weak as the minerals bonding disrupts, and new minerals formed [54].

In extremely strong rocks, the loss of strength between fresh (W0) and highly weathered (WIII) varieties may be as high as 80% [55]. The breaking of bonds between minerals and the development of microfractures are responsible for the loss in strength [56]. It is clear that the uniaxial compressive strength decreases gradually with an increase in the weathering state. Because of the reliability and consistency in the result, the uniaxial compressive strength has often been used for measuring the degree of weathering. Lumb [57] noticed that the strength depends on the mode of failure whether it is cataclastic or premature shear plane failure of the specimens.

Table 5. Relation between the rate of weathering and Unified Compressive Strength (UCS, Mpa) / Tensile Strength (TS, Ma) for the studied Bir El Beida metavolcanic rocks.

	UCS (Mpa)	Ts (Mpa)
W I	85	47
WII	72	33
WIII	38	13

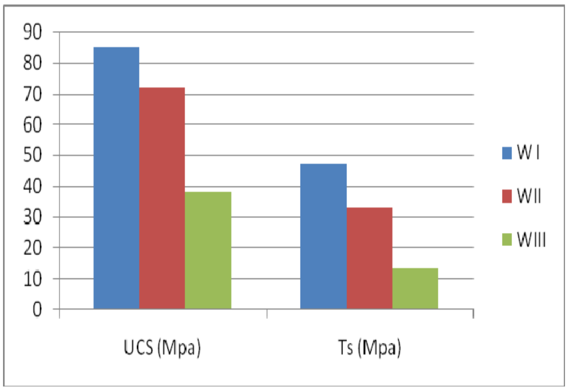

Figure 7. Unconfined Compressive Strength and Tensile Strength for the studied Bir El Beida metavolcanics.

The compressive aggregate strength is an important factor in the selection of rock aggregates. When determining the strength of normal concrete, most concrete paste is several times stronger than the components in concrete. According to ACI Committee [58], aggregate stress levels in concrete are often much higher than the average stress over the entire cross section of the concrete. Aggregate tensile strengths range from 2 to 15 MPa and compressive strengths range from 65 to 270 MPa. In the present study, metavolcanic rock aggregates at Bir El Beida were selected due to high strength character than the other rock types in Wadi Zareib. From the data of compressive and tensile strengths obtained in Table 5 and Figure 7, only WI and WII of El Beida metavolcanics agree the specification given by ACI Committee [58], promising to utilize in concrete. Uniaxial compressive strength is important parameter when rocks are used as concrete aggregates and base course material in high way construction. The selection of aggregates in concrete in Egypt is due to the rapid economic development and the growth in population [59-62].

8. Conclusions

From the above observations, it is likely concluded the following:

- Weathering is an essential process that affects the mechanical properties of rock material through chemical and physical weathering. Physical weathering leads to the opening of discontinuities by rock fractures, progressively breaking down the original rock. Chemical weathering results in chemical changes in the minerals. Both physical and chemical weathering greatly affects the engineering structures found at or near the Earth's surface. The composition of basalt is strongly influenced by the nature of weathering. In the field, the samples were described in terms of their weathering grade based on visual descriptions and a number of simple index tests. According to the developments of secondary minerals, percentages of ignition losses (L.O.I.), unified compression strength and tensile strength, the metavolcanic rocks in the area under study are classified into three types; slightly weathered (WI), moderately weathered (WII) and highly weathered (WIII). The WI and WII metavolcanics rock aggregates at Bir El Beida area are promising to be used as rock aggregates in concrete due to their higher compressive/tensile strength than the other weathering types in the study area.
- Chemically, weathering stage of the WII samples, which contain L.O.I. up to 7.38 wt. %, does not show a significant effect on the rock chemistry, especially on the concentrations of the immobile elements. Most elements redistributed in the newly formed secondary minerals (e.g. chlorite). The observed differences in the composition of the WII samples relative to the WI ones could be attributed to the fractional crystallization, original magmatic

features and/or crustal contamination. On the other hand, the major and trace elements in the highly weathered WIII samples and the pyroclastic deposits exhibit broad scatter in their abundances. This is largely assigned to both original rock composition and weathering process that caused element redistribution, mobilization and dilution. The geochemical characteristics of both localities indicate that they were erupted in an arc setting, and derived from a mantle source that was influenced by fluids, which are characteristic of subduction-related arc magmas. However, the most basic Wadi Zareib samples were generated from a more enriched mantle source as compared with those of Bir El Beida.

References

1. Gupta, A.S., Rao, K.S. Weathering indices and their applicability for crystalline rocks. Bulletin of Engineering Geology and the Environment, 2001, 60: 201- 221.
2. Gokceoglu, C., Zorlu, K., Ceryan, S., Nefeslioglu, H.A. A comparative study on indirect determination of degree of weathering of granites from some physical and strength parameters by two soft computing techniques. Materials Characterization, 2009, 60: 1317-1327.
3. Lee, S.G. Weathering and geotechnical characterization of Korean granites. Ph.D. thesis, Imperial College, University of London, 1987.
4. Hencher, S.R., Martin, R.P. The description and classification of weathered rocks in Hong Kong for engineering purposes. In Proceedings of the seventh Southeast Asian geotechnical conference, 1982: 125-142.
5. Irfan, T.Y., Powell, G.E. Engineering geological investigations for foundations on a deeply weathered granitic rock in Hong Kong. Bulletin of the International Association, 1985, 32: 67-80.
6. Raj, J.K. Characterization of weathering profile developed over a porphyritic biotite granite in Peninsula Malaysia. Bulletin of the International Association of Engineering Geology, 1985, 232: 121-130.
7. ISRM. Basic geotechnical description of rock masses. Int. Soc. for Rock Mech., Commission on Standardization of Laboratory and Field Tests. Int. J. Rock Mech. Min. Sci. Geomech. Abstr., 1981, 18: 85-110.
8. Anonymous. The description and classification of weathered for engineering purposes. Geological society engineering group working, Party report. Quartely Journal of Engineering Geology, 1995, 28: 207-242.
9. Irfan, T.Y. Mineralogy, fabric properties and classification of weathered granites in Hong Kong. Quarterly Journal of Engineering Geology, 1996, 29: 5- 35.
10. Gokceoglu, C., Aksoy, H. New approaches to the characterization of clay-bearing, densily jointed and weak rock masses. Engineering Geology, 2000, 58: 1-38.
11. Lan, H.X., Hu, R.L., Yue, Z.Q., Lee, C.F., Wang, S.J. Engineering and geological characteristics of granite weathering profiles in South China. Journal of Asian Earth Sciences, 2003, 21: 353- 364.
12. Akaad M.K., El Ramly M.F. Geological history and classification of the basement rocks of the Central Eastern Desert of Egypt. Geological Survey of Egypt, 1960, Paper no.9: 24p.
13. El-Sharkawy M.A., El- Bayoumi R. M. The ophiolites of Wadi Ghadir area, Eastern Desert, Egypt. Annals of Geological Survey of Egypt, 1979, 9: 125–135.
14. Dixon T.H. The evolution of continental crust in the Late Precambrian Egyptian Shield. Ph.D. Thesis, University of California at San Diego, 1979.
15. Nassef A.O., Bakor A.R., Hashad, A.H. Petrography of possible ophiolitic rocks along the Qift- Quseir road, Eastern Desert, Egypt. In: A.Al Shanti (Ed.), Evolution and mineralization of the Arabian-Nubian Shield, a symposium. Inst. Applied Geology (Jeddah) Bulletin, 1980, 3(4): 157–168.
16. Shackleton R.M. Precambrian tectonics of NE Africa. In: A. A. Al Shanti (ed.), Evolution and Mineralization of the Arabian- Nubian Shield, a Symposium. Inst. Applied Geology (Jeddah) Bulletin, 1980, 3(2): 1–6.
17. Ries A.C., Shackleton R.M., Graham R.H., Fitches, W.R. Pan-African structures, ophiolites and melange in the Eastern Desert of Egypt: a traverse at 26° N. Journal of Geological Society of London, 1983, 14: 75–95.
18. Abu El Ela, F.F. Bimodal volcanism of the Igla El Iswid-Um Khariga metavolcanics, Eastern Desert, Egypt. Egyptian Mineralogist, 1991, 3: 167–197.
19. Hashad A.H., Hassan M.A. On the validity of an Ensimatic Island, arc cratonization model to the evolution of the Egyptian Shield. Annals of Geological Survey of Egypt, 1979, 9: 70–80.
20. Engel A.E.J., Dixon T.H., Stern, R.J. Late Precambrian evolution of AfroArabian crust from ocean arc to craton. Geological Society of America Bulletin, 1980, 91: 699–706.
21. Abu El-Ela, F.F, Hassan M.A. Geology and geochemistery of bimodal volcanism north of Gabal Zabara, Eastern Desert, Egypt. Egyptian Journal of Geology, 1992, 36: 253–271.

22. Stern, R.J. Petrogenesis and tectonic setting of Late Precambrian ensimatic volcanic rocks, Central Eastern Desert of Egypt. Precambrian Research, 1981, 16: 197–232.
23. Moghazi A.M. Geochemistry and Petrogenesis of a high-K calc-alkaline Dokhan Volcanic suite, South Safaga area, Egypt: the role of late Neoproterozoic crustal extension. Precambrian Research, 2003, 125: 161–178.
24. Khalil E. Ocean-arc to continental margin volcanics sequences of the Pan-African Precambrian belt, Egypt: "geochemical approach". Egyptian Journal of Geology, 1997, 41: 477–528.
25. El-Gaby, S., List, F.K., Tehrani, R. The basement complex of the Eastern Desert and Sinai. In: Said, R. (Ed.), The Geology of Egypt. A. A. Balkema, Rotterdam, 1990: 175–184.
26. Ali, K.A., Stern, R.J., Manton, W.I., Kimura, J.I., Khamees, H.A. Geochemistry, Nd isotopes and U–Pb SHRIMP dating of Neoproterozoic volcanic rocks from the Central Eastern Desert of Egypt: new insights into the 750 Ma crust-forming event. Precambrian Research, 2009, 171: 1–22.
27. Stern R.J., Johnson P.R., Kröner A., Yibas B. Neoproterozoic Ophiolites of the Arabian-Nubian Shield. In: Kusky, T. (Ed.), Precambrian Ophiolites. Elsevier, 2004: 95–128.
28. Khyamy, A.A. Mostafa, M.O., Mohamed, H.A., Abdel-Gawad, G.M., Azzam, H.M., Fath El B., Mohamed, M.H. Geology of the Qift El Quseir District, Central Eastern Desert, Egypt. EGSMA. Documentation center, Internal Report No.44/2003.
29. Gupta, A.S. Engineering behaviour and classification of weathered rocks. Ph. D. thesis submitted to Indian Institute of Technology, Delhi, 1997.
30. IAEG. Rock and soil descriptions for engineering geological mapping. Report by the IAEG Commission on Engineering Geological Mapping. Bull. Int. Assoc. Engng Geol., 1981, 24: 235-274.
31. ISRM. Basic geotechnical description of rock masses. Int. Soc. for Rock Mech., Commission on Standardization of Laboratory and Field Tests. Int. J. Rock Mech. Min. Sci. Geomech. Abstr., 1981, 18: 85-110.
32. Tugrul, A., Gürpinaro, O.A. proposed weathering classification for basalts and their engineering properties (Turkey). Bulletin of the international Association of Engineering Geology, 1997, 55: 139-149.
33. Shrivastava, G. Influence of Weathering on the Engineering Properties of Basalt near Indore, Madhya Pradesh. International Conference on Advances in Engineering & Technology, 2014: 18-22.
34. Polat A., Hofmann A.W. Alteration and geochemical patterns in the 3.7–3.8 Ga Isua greenstone belt, West Greenland. Precambrian Research, 2003, 126: 197–218.
35. Polat A., Appel P.W.U., Frei R., Pan Y., Dilek Y., Ordóñez-Calderón J.C., Fryer B., Hollis J.A., Raith J.G. Field and geochemical characteristics of the Mesoarchean (3075 Ma) Ivisaartoq greenstone belt, southern West Greenland: evidence for seafloor hydrothermal alteration in supra-subduction oceanic crust. Gondwana Research, 2007, 11: 69–91.
36. Basta F.F., Maurice A.E., Bakhit, B.R, Ali K.A., Manton W.I. Neoproterozoic contaminated MORB of Wadi Ghadir ophiolite, NE Africa: Geochemical and Nd and Sr isotopic constraints. Journal of African Earth Sciences, 2011, 59: 227–242.
37. Sun, S., McDonough, W.F. Chemical and isotopic systematics of the oceanic basalts: implications for mantle composition and processes. Magmatism in the Ocean Basins. In: Saunders, A.D., Norry, M.J. (Eds.), Geological Society of London, Special Publications, 1989, 42: 313–345.
38. Pearce J., Cann J.R. Tectonic setting of basic volcanic rocks determined using trace element analyses. Earth and Planetary Science Letters, 1973, 19: 290–300.
39. Wood, D.A. The application of a Th–Hf–Ta diagram to problems of tectonomagmatic classification and establishing the nature of crustal contamination of basaltic lavas of the British Tertiary volcanic province. Earth and Planetary Science Letters, 1980, 50: 11–30.
40. Pearce J.A. Geochemical evidence for the genesis and eruptive setting of lavas from Tethyan ophiolites. Proc Intern ophiolite Symp, Nicosia, Cyprus, 1980: 261–272.
41. Straub S.M. Contrasting compositions of Mariana Trough fallout tephra and Mariana Island arc volcanics; a fractional crystallization link. Bulletin of Volcanology, 1995, 57: 403–421.
42. Ali K.A., Stern R.J., Manton W.I. , Kimura J., Whitehouse M.J., Mukherjee S.K. , Johnson P.R. , Griffin W.R. Geochemical, U–Pb zircon, and Nd isotope investigations of the Neoproterozoic Ghawjah Metavolcanic rocks, Northwestern Saudi Arabia. Lithos, 2010, 120: 379–392.
43. Smith I.E.M., Worthington T.J., Price R.C., Stewart R.B., Maas R. Petrogenesis of dacite in

an oceanic subduction environment: Raoul Island, Kermadec arc. Journal of Volcanology and Geothermal Research, 2006, 156: 252–265.
44. Green N.L. Influence of slab thermal structure on basalt source regions and melting conditions: REE and HFSE constraints on from the Garibaldi volcanic belt, northern Cascadia subduction system. Lithos, 2006. 87: 23–49.
45. Abd El-Rahman Y., Polat A., Dilek Y., Fryer B.J., El-Sharkawy M., Sakran S. Geohemistry and tectonic evolution of the Neoproterozoic incipient arc-forearc crust in the Fawakhir area, Central Eastern Desert of Egypt. Precambrian Research, 2009, 175: 116–134.
46. Pearce J.A. Geochemical finger printing of oceanic basalts with applications to ophiolite classification and the search for Archean oceanic crust. Lithos, 2008, 100: 14–48.
47. Hartley, A. A review of the geological factors influencing the mechanical properties of road surface aggregation. Quart. J. Eng. Geol., 1974, 7: 69-100.
48. Olsson, W.A. Grain size dependance on yield stress in marble. J. Geophys. Res., 1974, 79 (32): 4859-4861.
49. Fahy, M.P., Guccione, M.J. Estimating strength of sandstones using petrographic thin-section data. Bull. Assoc. Eng. Geol., 1979, 16 (4): 467-485.
50. Howarth, D.F., Rowlands, J.C. Development of an index to quantify rock texture for qualitative assessment of intact rock properties. Geotech. Testing J., 1986, 9 (4): 169-179.
51. Shakoor, A., Bonelli, R.E. Relationship between petrographic characteristics, engineering index properties, and mechanical properties of selected sandstones. Bull. Assoc. Eng. Geol., 1991, 28: (1), 55-71.
52. Haney, M.G., Shakoor, A. The relationship between tensile and compressive strengths for selected sandstones as influenced by index properties and petrographic characterestics. Proc. 7th Int. IAEG Cong., Lisbon, Portugal, 1994, 4: 3013-3021.
53. Hussin, A., Poole, C. The intragranular textures of aggregates and its correlation to the physical properties. Sains Malaysiana, 2010, 39 (1): 39-43.
54. Anon. The description and classification of weathered rocks for engineering purposes. Engineering Group Working party Report (Geol. Soc. London). Q. J. Engng Geol., 1995, 28 (3): 207-242.
55. Dearman, W.R., Irfan, T.Y. Classification and index properties of weathered coarse grained granites from SW England". Proc. 3rd Int. Cong. IAEG, Madrid, 1978, 2 (2): 119-130.
56. Beavis, F.C. Rock weathering. Engineering Geology. Blackwell Scientific, Melbourne, 1985.
57. Lumb, P. Engineering properties of fresh and decomposed igneous rocks from Hong Kong. Engng Geol., 1983, 19: 81-94.
58. ACI Committee, Cement and Concrete Technology, ACI 116R-00, ACI Committee 116 Report, American Concrete Institute, Farmington Hills, Michigan, 2000, 73 p.
59. Ismail, A.I.M. and Sadek Ghabrial, D. Acidic Rocks as Aggregates in Concrete: Engineering Properties, Microstructures and Petrologic Characteristics, Geotech Geol Eng, 2009, 27:519–528.
60. Ismail, A.I.M., Elmaghraby, M.S. and Mekky, H. Engineering Properties, Microstructure and Strength Development of Lightweight Concrete Containing Pumice Aggregates, Geotech Geol Eng, 2013, 31:1465–1476.
61. Ismail, A.I.M. and Darwish, H. Engineering Behaviour of Waste Glass as Aggregates in Concrete Containing Sand and Gravels, Intercerm, 2014, 63 (1-2): 45-48.
62. Ismail, A.I.M., Mekky, H., Elmaghraby, M.S. Assessment and utilization of some Egyptian clay deposits for producing lightweight concrete, International Journal of Materials Science and Applications, 2014, 3 (3): 79-83.

9/10/2014